ELSEVIER

Surface Science 367 (1996) 261–275

surface science

Linear sliding friction: on the origin of the microscopic friction for Xe on silver

B.N.J. Persson *, A. Nitzan [1]

Institut für Fesktörperforschung, Forschungszentrum Jülich, D-52425 Jülich, Germany

Received 21 February 1996; accepted for publication 17 May 1996

Abstract

We have performed a computer simulation study of the force required to slide xenon monolayer and bilayers on a silver surface. With information about the adsorbate–substrate interaction potential deduced from experimental data, we find that for the compressed incommensurate monolayer film the observed sliding friction is very close to the parallel microscopic friction which acts on the individual adsorbates, which is of mainly electronic origin. For the bilayer film a small fraction of the observed sliding friction may arise from internal excitations in the film, and the rest from the direct energy transfer to the substrate via the electronic friction.

Keywords: Atomistic dynamics; Computer simulations; Friction; Models of non-equilibrium phenomena

1. Introduction

The sliding of lubricated surfaces has been studied for many years [1], but the microscopic origin of the friction is not well understood. During sliding at low velocities, the lubrication fluid will be squeezed out from the contact areas between the two solids, but usually one or a few monolayers of lubrication molecules will be trapped between the surfaces (boundary lubrication) [2,3]. If the lateral corrugation of the adsorbate–substrate interaction potential is weak, as is typically the case for saturated hydrocarbons, then during sliding the molecules will slip relative to the surfaces. One important problem in sliding friction is to understand the origin and magnitude of the friction force acting on the individual molecules during slip. If the adsorbate velocity v is much smaller than the sound velocity and (for a metallic substrate) the Fermi velocity of the substrate, then the friction force acting on a molecule is proportional to the velocity [4]

$$\boldsymbol{F}_{\mathrm{f}} = -M\eta\boldsymbol{v}.$$

The microscopic friction η is assumed to be a diagonal matrix of the form

$$\eta = \begin{pmatrix} \eta_{\parallel} & 0 & 0 \\ 0 & \eta_{\parallel} & 0 \\ 0 & 0 & \eta_{\perp} \end{pmatrix}$$

where $\parallel$ and $\perp$ refer to motion parallel and perpendicular to the surface, respectively. For insulating surfaces (e.g. most metal oxides) the friction η can

* Corresponding author. Fax: +49 2461 612850; e-mail: iff083@zam001.kfa-juelich.de

[1] Permanent address: School of Chemistry, Tel Aviv University, Tel Aviv, 69978 Israel.

PII S0039-6028(96)00814-X

only be due to phonon emission but on metallic surfaces both electronic and phononic friction occur.

Information about the friction parameter η can be deduced from infrared spectroscopy [5] and inelastic helium scattering [6] measurements, since η determines the line width of adsorbate vibrations if inhomogeneous broadening and pure dephasing processes can be neglected. Information about η can also be deduced from quartz crystal microbalance (QCM) measurements. In the measurements by Krim et al. [7] two sides of a quartz crystal was covered by thin silver or gold films. When a voltage is applied to the crystal it performs in-plane oscillations. If adsorbates are adsorbed on the metal film the resulting mass-load will decrease the resonance frequency of the QC oscillator. But Krim et al. also observed an increased damping of the QC oscillator which can only result if, due to the inertia force, the adsorbates slides relative to the metal surface. If the pinning by the corrugated substrate potential can be neglected then from the adsorbate-induced change in the resonance frequency and damping of the QC oscillator, one can deduce both the adsorbate concentration and the damping $\eta_\parallel$. Finally, for metals, the electronic contribution to the friction $\eta_\parallel$ can be deduced from surface resistivity measurements [8,9]. In these measurements the adsorbate-induced change ΔR of the resistivity of a thin metallic film is measured. It is easy to prove that $\Delta R \propto \eta_\parallel$ by equalizing the ohmic energy dissipation with the frictional energy dissipation calculated in a reference frame moving with the drift velocity of the conduction electrons [9].

In this paper we present a computer simulation study of the force required to slide xenon monolayers and bilayers on a silver surface. With information about the adsorbate–substrate interaction deduced directly from experimental data, we find that for the compressed incommensurate (IC) xenon monolayer the sliding friction $\bar{\eta}$ deduced from the simulations is very close to the parallel microscopic friction $\eta_\parallel$ (of electronic origin) which enters in the Langevine equation, while the sliding friction for the bilayer is about 20% larger. For monolayer coverage (and below), we find that the motion of the adsorbates perpendicular to the surface is irrelevant, and a 2D model gives nearly the same result for the sliding friction as a 3D model.

In the light of our theoretical results we discuss the recent QCM measurements by Krim and Daly [10] of the sliding friction of monolayers and bilayers of Xe on Ag(111). We conclude that for the monolayer film the observed sliding friction $\bar{\eta}$ is nearly completely due to the direct coupling to the substrate via the friction $\eta_\parallel$, which is mainly of electronic origin. For the bilayer film a small fraction of the observed sliding friction may arise from internal excitations in the film, and the rest from the direct energy transfer to the substrate via the electronic friction.

These conclusions differ from those of Cieplak et al. [11], who claim that the observed friction force for all coverages is due to energy transfer into internal degrees of freedom (lattice vibrations) of the adsorbate layer, and that the nature of the dissipative adsorbate–substrate coupling is irrelevant. In particular, they put $\eta_\parallel = 0$, i.e. they only included the perpendicular friction. Our earlier results [4] and the present study cast doubt on this procedure, at least for low-corrugation surfaces. In particular, for the Xe/Ag system studied here, we have found that for the compressed incommensurate solid monolayer film, the sliding friction equals $\eta_\parallel$ to a very good approximation.

In this paper we measure angular frequency and damping in units of s^{-1} or cm^{-1}. The latter unit can be obtained from the former by multiplying with the factor $1/2\pi c = 5.309 \times 10^{-12}$ s cm^{-1}, where c is the light velocity.

2. Quartz crystal microbalance study of Xe on silver

The quartz crystal microbalance (QCM) has been used for decades for microweighing purposes, and was adapted for friction measurements by Krim and Widom, [12]. A QCM consists of a single crystal of quartz which oscillates in transverse shear motion (see Fig. 1). If the driving power for the QCM oscillator is switched off at time $t=0$, the amplitude of oscillation decays as

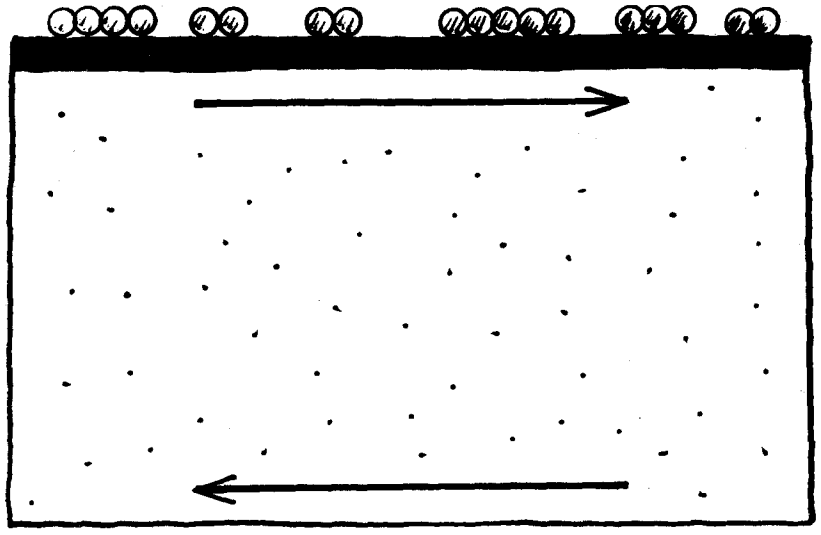

Fig. 1. A quartz crystal microbalance (QCM). The surface of the QCM is covered by a thin metallic film with adsorbates. During the QCM vibrations the adsorbate layer slides relative to the metal film, giving rise to energy dissipation and a damping of the QCM oscillator.

an exponentially damped sinusoidal

$$u = u_0 \cos(\omega_0 t)\, e^{-\gamma_0 t/2},$$

where ω_0 is the resonance frequency and γ_0 the damping of the oscillator. If a layer of adsorbates is deposited on one side of the QCM, this will result in a frequency shift $\Delta\omega$ and an increase in the damping $\Delta\gamma$, which can both be measured [13].

Krim and Daly have performed QCM measurements for Xe adsorbed onto the surface of silver film electrodes which were evaporated onto quartz crystals. The measurements were performed at $T=$ 77.4 K, where a thick Xe film would be in a solid state (the bulk melting temperature of Xe is 161 K). For a solid Xe slab adsorbed on the QCM surface, the frequency shift and the damping are given by [14]

$$\Delta\omega = -\frac{N_1 m}{M}\frac{\omega\bar{\eta}^2 P_1}{\omega^2+(\bar{\eta}P_1)^2}, \tag{1}$$

and

$$\Delta\gamma = \frac{2N_1 m}{M}\frac{\omega^2\bar{\eta}}{\omega^2+(\bar{\eta}P_1)^2}, \tag{2}$$

where N_1 is the number of adsorbates in the first layer in direct contact with the substrate, and $P_1 = N_1/N$ is the fraction of the adsorbates in the first layer. For coverage up to monolayer coverage $N_1 = N$ and $P_1 = 1$. Note that Eqs. (1) and (2) give

$$\Delta\gamma/\omega_0 = -2\Delta\omega/P_1\bar{\eta}. \tag{3}$$

Krim et al. have defined the slip time $\tau = 1/P_1\bar{\eta}$ so that

$$\Delta\gamma/\omega_0 = -2\Delta\omega\tau. \tag{4}$$

The sliding friction $\bar{\eta}$ is defined as follows. Consider an adsorbate layer on a substrate. If the adsorbate layer moves relative to the substrate there will be frictional stress σ acting on the adsorbate layer from the interaction with the substrate and given by $\sigma = n_a m\bar{\eta}v$, where v is the drift velocity of the adsorbate layer and n_a is the number of adsorbates per unit area in the first layer, in direct contact with the substrate. Eqs. (1) and (2) are not valid for a thick fluid layer, where additional energy dissipation will arise from the viscosity of the fluid. However, in the present case the adsorbate slab is in a solid state and all energy dissipation is assumed to be derived from the adsorbate–substrate interaction.

Suppose an adsorbate layer is sliding on a substrate. In the steady state the energy pumped

into the adsorbate layer by the external force must ultimately be transferred to the substrate. This can occur in two different ways (see Fig. 2). First (case (a)), there is a direct energy transfer from the center of mass motion of the adsorbate layer to the substrate. Secondly (case (b)), due to the lateral corrugation of the adsorbate–substrate interaction potential, during sliding energy will be transferred into internal degrees of freedom (lattice vibrations) of the adsorbate layer. If the adsorbate–substrate interaction is weak, the latter energy may be completely thermalized in the overlayer before it is finally transferred to the substrate. (Note: if the energy input is completely thermalized in the film before being transferred to the substrate then the temperature of the film T^* will be slightly higher than the substrate temperature T. In steady state, the temperature increase T^*-T will be determined by the condition that the power transferred to the adsorbate film from the external force F equals the energy transfer from the film to the substrate, which can be written as $\alpha(T^*-T)+m\eta_\parallel\langle v\rangle^2$, where the heat transfer coefficient $\alpha=k_B(2\eta_\parallel+\eta_\perp)$ (see Ref. [5]). Using this result, in Ref. [4] it is shown that the temperature increase can be written as $T^*-T=(F^2/mk_B\bar{\eta})(1-\eta_\parallel/\bar{\eta})/(2\eta_\parallel+\eta_\perp)$. In the present case the force of inertia is extremely weak (see estimate below), $F\approx 10^{-9}$ eV Å^{-1}, and if $1-\eta_\parallel/\bar{\eta}=0.5$ then we get $T^*-T\approx 10^{-9}$ K, i.e. completely negligible. For the incommensurate monolayer film the temperature increase is even smaller, since in this case $1-\eta_\parallel/\bar{\eta}$ is much smaller than 0.5). In a recent work by Cieplak et al. [11] it is claimed that only the second process (b) is important and that the nature of frictional coupling between the adsorbate layer and the substrate is irrelevant for the sliding dynamics. This conclusion is opposite to what we have found earlier [4], and also in the present work where, in fact, the sliding friction for the IC solid monolayer is nearly completely determined by process (a).

The force of inertia which acts on the adsorbate slab in a QCM measurement (which is the origin of why the slab will slide relative to the substrate) is extremely small, at least for thin adsorbate layers. This is the basis for the linear response assumption implicit in the theory behind Eqs. (1) and (2). To prove that the linear response assumption is an excellent approximation, note that the force of inertia acting on an adsorbate $F_{ext}\approx mA\omega^2{}_0$, where A is the vibration amplitude and ω_0 is the vibration frequency of the quartz crystal. Using $A\approx 100$ Å and $\omega_0\approx 10^8$ s^{-1} gives $F_{ext}\approx 10^{-9}$ eV Å^{-1}, which is extremely small compared with the force due to the corrugated substrate potential, which is of the order of U_0/a, where $a\approx 1$ Å is the substrate lattice constant and $U_0\approx 1$ meV is the amplitude of the lateral corrugation of the potential energy surface. Thus $U_0/a\approx 10^{-3}$ eV Å$^{-1}\gg F_{ext}$, and the linear response approximation is very accurate.

Fig. 3 shows the slip time as a function of coverage for Xe on Ag(111), where monolayer coverage is defined as 0.0597 Xe atoms per Å^2 (this is the highest possible density of Xe atoms in the

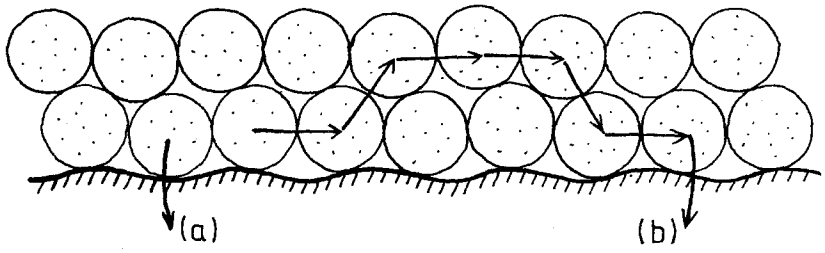

Fig. 2. An Xe bilayer sliding on a surface. Two processes contribute to the friction force acting on the bilayer. In (a), a direct process occurs where the kinetic energy of the translational motion of the bilayer is directly transferred to the substrate via the microscopic friction acting on the first layer of adsorbates in direct contact with the substrate. This energy transfer channel occurs also for an energetically perfectly smooth substrate surface (i.e. semi-infinite jellium model). Process (b) is an indirect process where the corrugated substrate potential excites vibrations in the bilayer (virtual phonons). These vibrational modes may thermalize before the energy is finally transmitted to the substrate via the same microscopic friction which determines the direct adsorbate–substrate energy transfer (channel (a)).

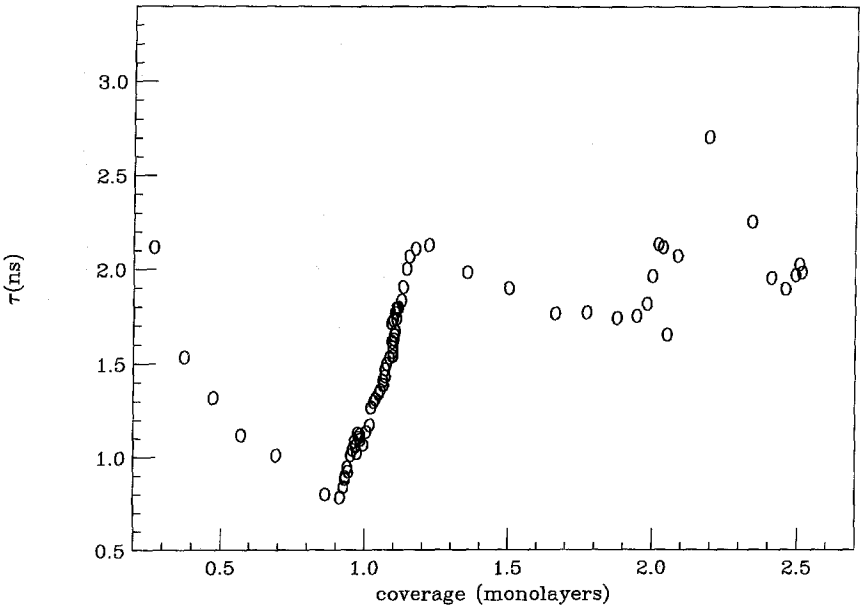

Fig. 3. Slip time τ as a function of coverage (1 monolayer = 0.0597 Å^{-2}) for Xe on Ag(111). From Ref. [10].

first layer in direct contact with the substrate). The slip times of the monolayer and bilayer Xe–films are $\tau = 1.19 \pm 0.04 \times 10^{-9}$ s and $1.87 \pm 0.07 \times 10^{-9}$ s, respectively, corresponding to the sliding friction $\bar{\eta} = 8.4 \pm 0.3 \times 10^{8}$ s^{-1} and $10.7 \pm 0.4 \times 10^{8}$ s^{-1}, respectively. The slip times at low adsorbate coverage tend to vary from one silver substrate to another indicating that surface imperfections may have a strong influence on the sliding dynamics at low coverage. However, the sliding friction for the monolayer and the bilayer films are very reproducible indicating that the pinning centers have a negligible influence on the sliding dynamics of these layers, and we mainly focus on these limiting cases below.

3. Model

Consider an adsorbate system and assume that in addition to the periodically corrugated adsorbate–substrate potential $U = \Sigma_i u(\boldsymbol{r}_i)$ and the adsorbate–adsorbate interaction potential $V = \frac{1}{2}\Sigma'_{ij} v(\boldsymbol{r}_i - \boldsymbol{r}_j)$, an external force $\boldsymbol{F}$ acts on each of the adsorbates. This will lead to a drift motion so that $mN_1\bar{\eta}\langle\dot{\boldsymbol{r}}\rangle = N\boldsymbol{F}$, where $\langle \ldots \rangle$ stands for thermal average, and where $\boldsymbol{r}$ denotes the coordinate of an arbitrary adsorbate. N_1 and N denote the number of adsorbates in the first layer in direct contact with the substrate and the total number of adsorbates, respectively. For coverage up to monolayer coverage $P_1 = N_1/N = 1$, but for higher coverage, $P_1 < 1$. This definition of $\bar{\eta}$ assumes that for coverage beyond monolayer coverage, the adsorbate system is in a solid state so that no (or negligible) energy dissipation occurs as a result of internal friction in the adsorbate system, e.g. due to the viscosity of a fluid slab. For a weak external force $\boldsymbol{F}$, the sliding friction $\bar{\eta}$ is independent of $\boldsymbol{F}$; this is the linear response limit directly relevant for the interpretation of QCM measurements.

We consider adsorbates on a (100) surface of an fcc crystal, but the general results emphasized below should be independent of the substrate lattice structure and of the detailed form of U and V. The equations of motion for the particle coordinate $\boldsymbol{r}_i(t)$ is taken to be

$$m\ddot{\boldsymbol{r}}_i + m\eta\dot{\boldsymbol{r}}_i = -\frac{\partial U}{\partial \boldsymbol{r}_i} - \frac{\partial V}{\partial \boldsymbol{r}_i} + \boldsymbol{f}_i + \boldsymbol{F}, \tag{5}$$

where $\boldsymbol{F}$ is the external force introduced above,

and f_i is a stochastically fluctuating force which describes the influence on particle i from the irregular thermal motion of the substrate. η is a diagonal matrix of the form

$$\eta = \begin{pmatrix} \eta_\parallel & 0 & 0 \\ 0 & \eta_\parallel & 0 \\ 0 & 0 & \eta_\perp \end{pmatrix}. \quad (6)$$

The components of f_i^α and f_i are related to the friction η via the fluctuation-dissipation theorem

$$\langle f_i^\alpha(t) f_j^\beta(0)\rangle = 2mk_B T\eta_{\alpha\beta}\delta_{ij}\delta(t). \quad (7)$$

The friction $\eta_\perp$ associated with motion normal to the surface is usually much larger than the parallel friction $\eta_\parallel$. Note also that η depends on the adsorbate–substrate separation and on the position of the adsorbates along the surface. However, in the present case, because of the low temperature and the weak lateral corrugation of the adsorbate–substrate interaction potential, all the adsorbates in the first monolayer will, to an excellent approximation, experience the same friction η. Since the adsorbate–substrate interaction is very short ranged, for multilayer adsorption, to a good approximation the friction η vanishes for all adsorbates except for those in the first layer in direct contact with the substrate. Thus, for the Xe bilayer case studied below we take $\eta = 0$ for the Xe atoms in the second layer (more accurately, we assume that η switches from a constant non zero value for $z < z_1$ to zero for $z > z_1$, where z_1 is the z-coordinate in the middle between the first and second layer; in reality η changes smoothly with z, but since well-defined Xe layers are formed, with essentially zero probability to find an adsorbate between two layers (see Fig. 5 below), both prescriptions should give identical results).

The adsorbate–substrate interaction potential is taken to be

$$u(\boldsymbol{r}) = E_B\left[e^{-2\alpha(z-z_0)} - 2\,e^{-\alpha(z-z_0)}\right] + U_0\left[2-\cos(kx)-\cos(ky)\right]e^{-\alpha'(z-z_0)}, \quad (8)$$

so that $2U_0$ is (approximately) the activation barrier for diffusion and $k = 2\pi/a$, where a is the lattice constant of the substrate. The adsorbate binding energy E_B has been measured experimentally for many adsorbate systems, and α can be deduced from the vibration frequency for the perpendicular adsorbate–substrate vibrational mode. Writing $z = z_0 + q$, where q is the perpendicular vibrational normal mode coordinate, we get to quadratic order in q: $u \approx E_B\alpha^2 q^2$. This must equal $M\omega_\perp^2 q^2/2$, where $\omega_\perp$ is the vibrational resonance frequency of the perpendicular vibration. Hence

$$\alpha = \left(\frac{M\omega_\perp^2}{2E_B}\right)^{1/2}.$$

For Xe on silver, $\omega_\perp \approx 22\ \mathrm{cm}^{-1}$ and $E_B \approx 0.23$ eV, which gives $\alpha = 0.72\ \text{Å}^{-1}$. In the simulations presented below we have also taken $\alpha' = 0.72\ \text{Å}^{-1}$. Similarly, from a knowledge of the resonance frequency $\omega_\parallel$, it is possible to estimate the barrier height $2U_0$. Using Eq. (8) we get $U_0 = M\omega_\parallel^2/k^2$. The frequency $\omega_\parallel$ has not been measured for Xe on Ag(100) (or Ag(111)), but it has been measured [15] using inelastic helium scattering for the $(\sqrt{3}\times\sqrt{3})$ Xe structure on Cu(111) where at the zone center $\omega_\parallel = 3 \pm 1\ \mathrm{cm}^{-1}$. In the calculations reported in this paper we have used $\omega_\parallel = 2.7\ \mathrm{cm}^{-1}$ corresponding to $2U_0 = 1.9$ meV.

The friction parameters $\eta_\parallel$ and $\eta_\perp$ can be estimated as follows. Consider first the phonon contribution to the friction. If the characteristic frequency of the forces exerted on the substrate by the motion of the adsorbate is well below the maximum phonon frequency (or the Debye frequency) of the substrate, which usually is the case for physisorption systems, then the phononic friction can be calculated using the elastsic continuum model. This gives [16]

$$\eta_\perp \approx \frac{3}{8\pi}\frac{M}{\rho}\left(\frac{\omega_\perp}{c_T}\right)^3\omega_\perp, \quad (9)$$

and

$$\eta_\parallel \approx \frac{3}{8\pi}\frac{M}{\rho}\left(\frac{\omega_\parallel}{c_T}\right)^3\omega_\parallel. \quad (10)$$

For Xe on silver with $\omega_\perp \approx 22\ \mathrm{cm}^{-1}$ and $\omega_\parallel \approx 2.7\ \mathrm{cm}^{-1}$, these equations give $\eta_\perp = 2.5\times10^{11}\ \mathrm{s}^{-1}$ and $\eta_\parallel = 5.5\times10^{7}\ \mathrm{s}^{-1}$.

The phononic frictions $\eta_\perp$ and $\eta_\parallel$ calculated above for isolated adsorbates should also be good approximations for fluid adsorbate layers. However, for perfect IC solid adsorbate layers, the phononic friction is expected to vanish [17,18]. Real surfaces always have imperfections, so that in practice the phononic friction is always finite, but for incommensurate structures it may be much smaller than predicted by Eqs. (9) and (10). In the applications below we find that the electronic friction is much more important than the phononic friction, and since the electronic friction varies relatively little with the coverage (in particular, it does not vanish at incommensurate coverage) the uncertainty in the value for the phononic friction is of no practical importance.

The parallel electronic friction has been estimated from surface resistivity measurements as well as from theoretical calculations; both theory and measurements give the electronic contribution to $\eta_\parallel$ to be of the order $\sim 5\times 10^8$ s^{-1}, which is about one order of magnitude larger than the estimated (low-coverage) phononic contribution to $\eta_\parallel$. On the other hand, for fluid adsorbate layers the electronic contribution to $\eta_\perp$ is negligible compared with the phononic contribution.

The adsorbate–adsorbate interaction potential V is taken as a sum of Lennard-Jones pair potentials

$$v(r)=\epsilon\left[\left(\frac{r_0}{r}\right)^{12}-2\left(\frac{r_0}{r}\right)^{6}\right], \tag{11}$$

where ϵ is the well depth and r_0 to the particle separation at the minima in the pair potential. For Xe we have used $\epsilon=19$ meV and $r_0=4.54$ Å. We have chosen a to correspond to Xe on Ag(100); in this case $a=b/\sqrt{2}=2.89$ Å (where b is the lattice constant of Ag) so that $r_0/a\approx 1.56$. Table 1 summarizes the parameter values used below, unless otherwise stated.

Table 1
The parameter values used in the simulations unless otherwise stated

$\omega_\perp=22$ cm^{-1}	$\omega_\parallel=2.7$ cm^{-1}
$E_0=0.23$ eV	$\alpha=0.72$ Å^{-1}
$U_0=0.95$ meV	$\alpha'=0.72$ Å^{-1}
$\epsilon=19$ meV	$r_0=4.54$ Å
$a=2.89$ Å	$\eta_\perp=2.5\times 10^{11}$ s^{-1}

Eq. (5) describes the motion of an adsorbate system on a corrugated substrate. When the external force $\boldsymbol{F}=0$ a particle performs irregular motion (diffusion) with no long-time drift, i.e. $\langle \boldsymbol{r}_i\rangle=0$. For $\boldsymbol{F}>0$, in addition to the irregular motion, the particles drift in the direction of $\boldsymbol{F}$ with the speed $\langle \dot{\boldsymbol{r}}\rangle=\boldsymbol{F}/m\bar{\eta}$. Note that when $U_0=0$, the thermal average of Eq. (5) gives

$$m\langle \ddot{\boldsymbol{r}}\rangle+m\eta_\parallel\langle \dot{\boldsymbol{r}}\rangle=\boldsymbol{F},$$

or, since $\boldsymbol{F}$ is constant,

$$m\eta_\parallel\langle \dot{\boldsymbol{r}}\rangle=\boldsymbol{F},$$

so that $\bar{\eta}=\eta_\parallel$, as expected in this limiting case.

We have obtained the sliding friction $\bar{\eta}$ from computer simulations based on the Langevin Eq. (5). The stochastic forces $\boldsymbol{f}_i$ are assumed to be uncorrelated Gaussian random variables and are generated by a standard procedure [19]. The time variable was discretized with the step length $\Delta=0.01\tau$ (where the natural time unit $\tau=r_0(m/\epsilon)^{1/2}$) and the integration routine described by Tully et al. [20] was used in all the simulations. The basic unit was chosen as a square containing $M\times M$ substrate atoms, where typically $M=12$. In the snapshot pictures of adsorbate structures shown below, it is assumed that the hollow sites have the largest adsorbate–substrate binding energy, i.e. these sites correspond to the local minima of $u(\boldsymbol{r})$ given by Eq. (8). In N denotes the number of adsorbates in the basic unit, then the coverate $\theta=N/(M\times M)$. In all simulations periodic boundary condition have been used. The system was "thermalized" by $\sim 10^6$ time steps which correspond to the actual "preparation" time $10^4\tau$; this was enough in all cases in order to reach thermal equilibrium. The drift friction $\bar{\eta}$ was obtained from the simulations using the definition $\bar{\eta}=F/mP_1\langle v\rangle$, where F is a weak external force acting in the x direction on each adsorbate and which results in the adsorbate drift velocity $\langle v\rangle$, which was obtained from the simulations by averaging over all the particles in the basic unit and over many integration steps corresponding to the time $\sim 10^4\tau$.

4. Results

All results presented below have been obtained with the temperature $T=77.4$ K. Fig. 4 shows the number of adsorbates N_1, N_2 and N_3 in the basic unit cell, occupying the first, second, and third layers, respectively, as a function of the total number N of adsorbates. Note that all Xe atoms occupies the first layer for N up to 68 atoms in the 12×12 basic unit; for $N=69$ one Xe atom occupies the second layer. Thus the monolayer Xe coverage in the simulations correspond to $n_a=68/(144a^2)\approx 0.0565$ Å^{-2}. Close to the completion of the bilayer one additional Xe atom is transferred to the first monolayer giving a compressed layer with $n_a=0.0574$ Å^{-2}. Experimentally [21], at $T=77.4$ K, Xe condenses onto Ag(111) as an "uncompressed" solid monolayer with 0.05624 atoms per Å^2. The monolayer accommodates further atoms by compressing, until it reaches 0.0597 atoms per Å^2.

Fig. 5 shows the Xe-probability distribution $P(z)$ and the drift velocity $\langle v\rangle$ (arbitrary unit) as a function of the distance z from the surface for two different cases: (a) for one complete monolayer of Xe (coverage $\theta=68/144$) and (b) for the bilayer (132 particles in the basic unit). In both cases $P(z)$ is normalized so that

$$\int d(z/r_0)P(z)=1.$$

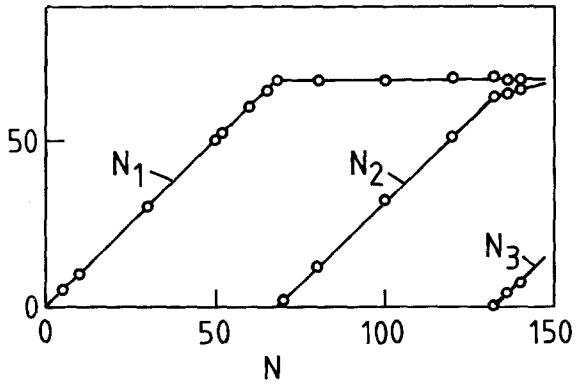

Fig. 4. The variation of the number of adsorbates in the first N_1, second N_2 and third N_3 Xe layers as a function of increasing number N of adsorbates in the basic unit cell. Note that the third layer starts to become populated before the second layer is completed.

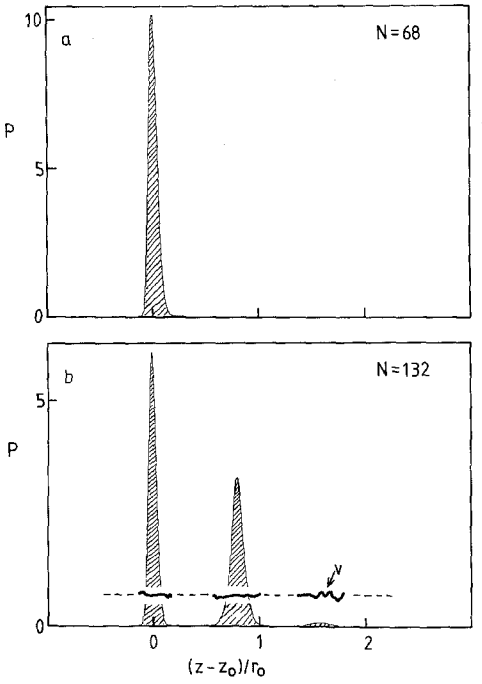

Fig. 5. (a) The probability distribution $P(z)$ of particles in the direction normal to the surface for one complete monolayer of Xe on Ag(100) (coverage $\theta=68/144$). (b) The same quantity for two monolayers (132 particles in the 12×12 cell). In both cases $P(z)$ is normalized so that the integral over all z equals unity. The horizontal wavy line in (b) shows the drift velocity v (arbitrary unit). In the calculation, $\eta_\parallel=6.2\times 10^8$ s^{-1} and the other parameters are as in Table 1.

In the calculation, $\eta_\parallel=6.2\times 10^8$ s^{-1}. Note that the Xe atoms form well-defined layers, and that the probability distribution $P(z)$ for the first layer is narrower than that of the second layer. This is, of course, related to the stronger Xe–substrate interaction as compared with the Xe–Xe interaction, which results in a higher frequency of the perpendicular Xe–substrate vibration as compared with the perpendicular Xe vibration of the second-layer Xe atoms. Note also that there is already a small occupation of the third layer before the second layer is fully occupied (see Fig. 4).

The horizontal wavy lines in Fig. 5 show the variation of the drift velocity with the center of mass position (normal to the surface) of the adsorbates. The fluctuations in the curves comes from the limited time-period over which the velocity has been averaged, and are particularly large in the

regions where the probability of finding a particle is low. It is clear that the drift velocity of the second (and higher) layer is identical to those of the first layer. This is true even when the second (or third) layer is incomplete, and simply reflects the fact that the lateral corrugation experienced by an Xe atom in the second (or third) layer is much higher than the (small) corrugation of the adsorbate–substrate interaction potential. Daly and Krim [10] have pointed out that since for the bilayer the second layer is perfectly commensurate with the first layer, the two move in unison while sliding. However, they also suggested that just beyond monolayer coverage, where a dilute "gas" of second-layer adsorbates occurs, the second-layer atoms slide relative to the first layer. However, our simulations shows that this effect is negligible at the low temperature which the experiments have been performed.

Fig. 6 shows snapshot pictures of the adsorbate layer in cases (a) and (b) in Fig. 5. As expected, the Xe monolayer forms a hexagonal structure which is incommensurate (IC) with respect to the substrate. In the bilayer case the second-layer atoms (filled circles) occupy the hollow sites in the first layer (the two arrows points at an Xe atom in the third layer occuping two hollow sites of the second layer).

Fig. 7 shows the dependency of $\eta_\parallel/\bar{\eta}$ on the coverage up to monolayer coverage. In the calculation, $\eta_\parallel = 2.5 \times 10^9\ s^{-1}$. Note the initial drop in $1/\bar{\eta}$ when going from the dilute lattice-gas state to the formation of small solid islands, and the increase of $1/\bar{\eta}$ close to the formation of the full monolayer phase. At monolayer coverage (68 Xe atoms in the unit cell) the sliding friction is nearly equal to $\eta_\parallel$.

Table 2 shows $\eta_\parallel/\bar{\eta}$ for the IC solid monolayer and the bilayer when $\eta_\parallel = 6.2 \times 10^8\ s^{-1}$. Note that for the monolayer film, $\bar{\eta}$ is equal to $\eta_\parallel$ within the accuracy of the simulation, while for the bilayer film, the sliding friction $\bar{\eta}$ is about 20% larger than $\eta_\parallel$.

5. Comparison with experiments

In the light of the theoretical results presented above, let us discuss the QCM experiments by

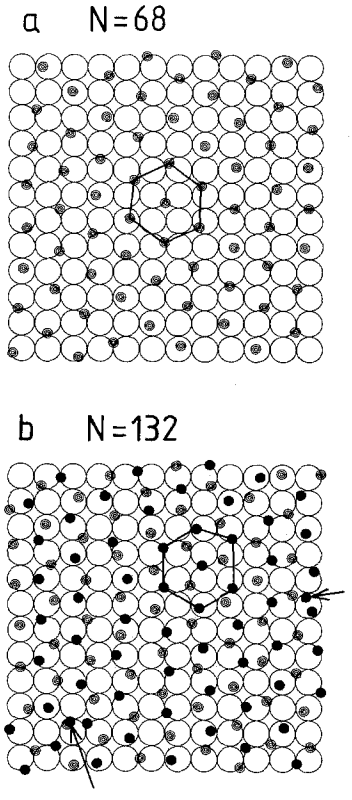

Fig. 6. Snapshot pictures for the adsorbate layer in cases (a) and (b) in Fig. 5.

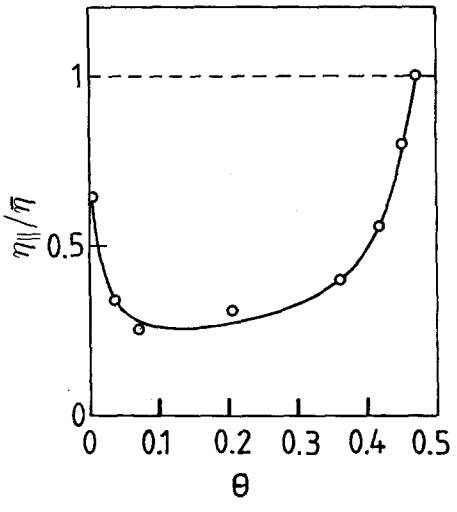

Fig. 7. The dependency of the inverse of $\eta_\parallel/\bar{\eta}$ on the coverage up to completion of the first Xe-monolayer. In the calculation, $\eta_\parallel = 2.5 \times 10^9\ s^{-1}$ and the other parameters are as in Table 1.

Table 2
The inverse of the normalized sliding friction, $\eta_\parallel/\bar{\eta}$, for an Xe monolayer and bilayer; in the calculation, $\eta_\parallel = 6.2 \times 10^8$ s^{-1}

System	$\eta_\parallel/\bar{\eta}$
Monolayer ($N=68$)	0.98 ± 0.04
Bilayer ($N=132$)	0.83 ± 0.02

Daly and Krim. The experimental data (see Fig. 3) are for the Xe/Ag(111) system while our simulations are for Xe on Ag(100). We have chosen to study the latter system because this system is easier to analyze analytically. Nevertheless, the qualitative results obtained above should also be valid for the Ag(111) surface. In particular, the sliding friction of the compressed IC solid monolayer system should be nearly equal to $\eta_\parallel$, i.e. a negligible contribution to the sliding friction from internal excitations in the film is expected. From Fig. 3 we obtain $\bar{\eta} = (8.4 \pm 0.3) \times 10^8$ s^{-1} for the monolayer film; this value is similar to the parallel electronic friction deduced from surface resistivity date [22], and is also in accordance with theoretical estimates [9,23] of the electronic friction. For an Xe bilayer on Ag(111) we have found that a small fraction (about 20%) of the sliding friction is due to internal excitations in the film. The observed sliding friction for the Xe/Ag(111) system is approximately 27% larger for the bilayer than for the monolayer film, i.e. of the same order of magnitude as we obtain in the simulations. Nevertheless, surface resistivity measurements [22] have shown that the electronic friction of a bilayer film may be about 20% larger than for the monolayer film; the observed increase in the sliding friction for the bilayer film may therefore result partly from internal excitations in the film, and partly from a slight increase in the electronic friction.

6. Analysis of the results of the computer simulation, and discussion

In this section we address the following fundamental question related to the simulations presented in Section 4.

Why is the sliding friction for the compressed IC solid monolayer essentially equal to the parallel friction $\eta_\parallel$, i.e. why is the contribution from the perpendicular motion unimportant and why is the contribution from internal excitations in the film (process (b) in Fig. 2) negligible?

Let us first discuss the relative importance of the "perpendicular" and "parallel" friction (see also Ref. [24]). We first derive a formally exact expression for $\bar{\eta}$. The power absorption (per adsorbate) P induced by the force $\boldsymbol{F}$ can be written in two different ways. First, from the definition of $\bar{\eta}$

$$P = \langle \boldsymbol{v} \cdot \boldsymbol{F} \rangle = \langle \boldsymbol{v} \rangle \cdot \boldsymbol{F} = m\bar{\eta} \langle \boldsymbol{v} \rangle^2. \tag{12}$$

Next, let us write the velocity of an adsorbate as

$$\boldsymbol{v} = \langle \boldsymbol{v} \rangle + \delta \boldsymbol{v},$$

where $\langle \delta \boldsymbol{v} \rangle = 0$. Now, in the steady state, the power P that the external force $\boldsymbol{F}$ "pumps" into the adsorbate layer must equal the energy transfer per unit time from the adsorbate layer to the substrate. The latter quantity is given by

$$\begin{aligned} P &= -\left(\langle \boldsymbol{v} \cdot \boldsymbol{F}_f \rangle - \langle \boldsymbol{v} \cdot \boldsymbol{f} \rangle \right) \\ &= m\eta_\perp \left(\langle \delta v_\perp^2 \rangle - \langle \delta v_\perp^2 \rangle_0 \right) \\ &\quad + m\eta_\parallel \left(\langle \delta v_\parallel^2 \rangle - \langle \delta v_\parallel^2 \rangle_0 \right) + m\eta_\parallel \langle \boldsymbol{v} \rangle^2, \end{aligned} \tag{13}$$

where $\boldsymbol{f}$ is the fluctuating force of Eq. (5), $\langle \ldots \rangle_0$ stands for thermal average when $\boldsymbol{F} = 0$, and where

$$\boldsymbol{F}_f = -m \left(\eta_\perp \boldsymbol{v}_\perp + \eta_\parallel \boldsymbol{v}_\parallel \right).$$

Combining Eqs. (12) and (13) gives

$$\begin{aligned} \bar{\eta} &= \eta_\perp \left(\langle \delta v_\perp^2 \rangle - \langle \delta v_\perp^2 \rangle_0 \right) / \langle \boldsymbol{v} \rangle^2 \\ &\quad + \eta_\parallel \left[\left(\langle \delta v_\parallel^2 \rangle - \langle \delta v_\parallel^2 \rangle_0 \right) / \langle \boldsymbol{v} \rangle^2 + 1 \right]. \end{aligned} \tag{14}$$

The relative importance of the contributions to $\bar{\eta}$ from the "perpendicular" and "parallel" friction for the IC solid monolayer film can be estimated as follows. Consider first the perpendicular term. As an adsorbate drifts with the velocity $\langle \boldsymbol{v} \rangle$ parallel

to the surface the distance of the adsorbate from the surface will fluctuate by the amount δz. We can obtain δz from the potential Eq. (8) by assuming that an adsorbate, as it translates along the surface, always occupies the position normal to the surface which minimizes the adsorbate–substrate interaction energy, i.e. by requiring $\partial u/\partial z = 0$. This gives $z = z_0 + \delta z$, where

$$\delta z = (U_0/2\alpha E_B)(2 - \cos kx - \cos ky).$$

The contribution to the perpendicular velocity by the drift motion parallel to the surface is therefore $\delta v_\perp = \delta \dot{z}$ or

$$\delta v_\perp = (kU_0 v/2\alpha E_B) \sin kx,$$

where we have assumed that the drift motion occurs along the x-axis with the speed v (i.e. $x = vt$). Thus

$$\left(\langle \delta v_\perp^2 \rangle - \langle \delta v_\perp^2 \rangle_0 \right) / \langle v \rangle^2 \approx \frac{1}{2} \left(\frac{kU_0}{2\alpha E_B} \right)^2. \tag{15}$$

For the Xe/Ag(100) system, the prefactor $\eta_\perp$ in Eq. (14) for $\bar{\eta}$ becomes $\sim 3 \times 10^{-5}$. The friction parameter $\eta_\perp$ has been estimated above using the elastic continuum model to be $\eta_\perp \sim 2.5 \times 10^{11}$ s^{-1}. Hence, the perpendicular contribution to $\bar{\eta}$ for Xe on Ag(100) is of the order of $\sim 7 \times 10^6$ s^{-1}. The contribution from the parallel friction to Eq. (14) for Xe on Ag(100) is of the order (see above) of $\sim 10^9$ s^{-1}. Thus, the parallel contribution to $\bar{\eta}$ is a factor of $\sim 10^2$ larger than the perpendicular contribution.

We have shown that the perpendicular adsorbate motion is unimportant at monolayer coverage. Our simulations shows that this is true also for coverages below monolayer. For example, in Table 3 we show the sliding friction for $\theta = 52/144$ for two different values of the decay constant α

Table 3
The inverse of the normalized sliding friction, $\eta_\parallel/\bar{\eta}$, for two different decay constants α; in the calculation, $N = 52$ and $\eta_\parallel = 2.5 \times 10^9$ s^{-1}

α (Å^{-1})	$\eta_\parallel/\bar{\eta}$
0.72	0.38 ± 0.03
1.98	0.40 ± 0.02

occurring in the potential $u(r)$ in Eq. (8). A large α implies that the particles cannot displace in the direction normal to the surface, i.e. the motion is nearly two-dimensional. We note that increasing α from 0.72 to 1.98 Å^{-1} leads to a negligible change in the sliding friction i.e. a strict 2D model gives nearly the same result for the sliding friction as the 3D model.

Next, let us discuss why there is a negligible contribution to the sliding friction from internal excitations in the film (see also Refs. [25,18]). We use a 2D model since we have just proven that the motion in the z-direction is unimportant. Let us write the coordinates for the particles in the IC solid sliding state as

$$\boldsymbol{r}_i = \boldsymbol{v}t + \boldsymbol{x}_i + \boldsymbol{u}_i, \tag{16}$$

where $\boldsymbol{v}$ is the drift velocity, $\boldsymbol{x}_i = (x_i, y_i)$ are the perfect lattice sites (in a reference frame moving with the velocity $\boldsymbol{v}$) of the hexagonal structure, and $\boldsymbol{u}_i$ is the (fluctuating) displacements away from these sites. Because of the weak corrugation of the substrate potential, $|\boldsymbol{u}_i|$ is small. Substituting Eq. (16) in Eq. (5) and expanding U and V to linear order in $\boldsymbol{u}_i$ gives

$$\begin{aligned} m\ddot{\boldsymbol{u}}_i + m\eta_\parallel \dot{\boldsymbol{u}}_i + \textstyle\sum_j K_{ij} \cdot \boldsymbol{u}_j \\ = \mathbf{f}_i - kU_0 \left[\hat{x} \sin k(v_x t + x_i) + \hat{y} \sin k(v_y t + y_i) \right] \\ - k^2 U_0 \left[\hat{x} u_{xi} \cos k(v_x t + x_i) \right. \\ \left. + \hat{y} u_{yi} \cos k(v_y t + y_i) \right] \\ + m(\bar{\eta} - \eta_\parallel)\boldsymbol{v}, \end{aligned} \tag{17}$$

where the force constant matrix K_{ij} has the components $K_{ij}^{\alpha\beta} = \partial^2 V / \partial u_i^\alpha \partial u_j^\beta$. To linear order in U_0 we obtain

$$\begin{aligned} m\ddot{\boldsymbol{u}}_i + m\eta_\parallel \dot{\boldsymbol{u}}_i + \sum_j K_{ij} \cdot \boldsymbol{u}_j \\ = \boldsymbol{f}_i - kU_0 \left[\hat{x} \sin k(v_x t + x_i) + \hat{y} \sin k(v_y t + y_i) \right]. \end{aligned} \tag{18}$$

Let us introduce the matrix $K(\boldsymbol{q})$ with the

components

$$K^{\alpha\beta}(\boldsymbol{q})=\sum_j K_{ij}^{\alpha\beta}\,\mathrm{e}^{-\mathrm{i}\boldsymbol{q}\cdot(\boldsymbol{x}_i-\boldsymbol{x}_j)},$$

or

$$K^{\alpha\beta}(\boldsymbol{q})=\frac{6\epsilon}{r_0^2}\sum_{n\neq 0}\left[\left(\xi_n^4-\xi_n^7\right)\delta_{\alpha\beta}+\left(14\xi_n^8-8\xi_n^5\right)\frac{x_n^\alpha x_n^\beta}{r_0^2}\right]\left(1-\mathrm{e}^{\mathrm{i}\boldsymbol{q}\cdot\boldsymbol{x}_n}\right),$$

where $\xi_n=r_0^2/\boldsymbol{x}_n^2$, and where the sum is over all the sites $\boldsymbol{x}_n$ of the hexagonal lattice of the adsorbate layer (excluding the site at the origin). Assume that $v=v\hat{x}$. If $\boldsymbol{e}_1$ and $\boldsymbol{e}_2$ ($\boldsymbol{e}_i\cdot\boldsymbol{e}_j=\delta_{ij}$) denote the longitudinal and transverse eigenvectors of $K(\boldsymbol{q})$ for $\boldsymbol{q}=(k,0)$, corresponding to the eigenvalues $m\omega_1^2$ and $m\omega_2^2$, respectively, and if we expand $\hat{x}=\alpha_1\boldsymbol{e}_1+\alpha_2\boldsymbol{e}_2$, then the solution to Eq. (18) can be written as

$$\boldsymbol{u}_i=(\boldsymbol{u}_i)_{\mathrm{T}}-\frac{kU_0}{m}\left(\boldsymbol{e}_1\frac{\alpha_1\sin(\omega t+x_i+\phi_1)}{\left[(\omega^2-\omega_1^2)^2+\omega^2\eta_\parallel^2\right]^{1/2}}+\boldsymbol{e}_2\frac{\alpha_2\sin(\omega t+x_i+\phi_2)}{\left[(\omega^2-\omega_2^2)^2+\omega^2\eta_\parallel^2\right]^{1/2}}\right),\tag{19}$$

where $\tan\phi_1=\omega\eta_\parallel/(\omega^2-\omega^2{}_1)$ and $\omega=kv$, and where $(\boldsymbol{u}_i)_{\mathrm{T}}$ is the thermal contribution to $\boldsymbol{u}_i$ derived from the random forces $\boldsymbol{f}_i$. Substituting Eqs. (19) in (17) and averaging over time gives

$$\bar{\eta}=\eta_\parallel+\frac{k^4U_0^2\eta_\parallel}{2m^2}\left[\frac{\alpha_1 e_{x1}}{(\omega^2-\omega_1^2)^2+\omega^2\eta_\parallel^2}+\frac{\alpha_2 e_{x2}}{(\omega^2-\omega_2^2)^2+\omega^2\eta_\parallel^2}\right].\tag{20}$$

In the present case $v\to 0$ so that $\omega\ll\omega_1$, ω_2, and Eq. (20) reduces to

$$\bar{\eta}=\eta_\parallel+\frac{k^4U_0^2\eta_\parallel}{2m^2}\left[\frac{\alpha_1 e_{x1}}{\omega_1^4}+\frac{\alpha_2 e_{x2}}{\omega_2^4}\right].\tag{21}$$

It is important to note the physical mechanism behind the two terms in Eq. (21). The first term describes the direct energy transfer to the substrate owing to the center of mass motion of the adsorbate system (process (a) in Fig. 1). The second term describes the transfer of energy from the center of mass motion into sound waves in the adsorbate system (process (b) in Fig. 1). This is caused by the corrugated substrate potential which exert an oscillating force on the (sliding) elastic 2D solid. In the analytical calculation above, the sound waves are only damped via the friction $\eta_\parallel$ which is very small. However, in a real system (and in the simulations), an additional damping of these sound waves comes from scattering against imperfections and from phonon–phonon collisions arising fron nonlinear terms in the expansion of the Xe–Xe interaction potential (not included in the analysis above). To account for these processes one must replace the damping $\eta_\parallel$ in the second term in Eq. (21) with a new damping $\eta_\parallel'=\eta_\parallel+\eta_\parallel''$, where $\eta_\parallel''$ has its origin in the scattering process described above.

$$\bar{\eta}=\eta_\parallel+\frac{k^4U_0^2\eta_\parallel'}{2m^2}\left[\frac{\alpha_1 e_{x1}}{\omega_1^4}+\frac{\alpha_2 e_{x2}}{\omega_2^4}\right].\tag{22}$$

It is convenient to write

$$\omega_1=\left(\frac{6\epsilon}{mr_0^2}\right)^{1/2}f_1(n_{\mathrm{a}}),\quad \omega_2=\left(\frac{6\epsilon}{mr_0^2}\right)^{1/2}f_2(n_{\mathrm{a}}),\tag{23}$$

where f_1 and f_2 are a dimensionless functions of the adsorbate coverage n_{a}. In Table 4 we give f_1 and f_2 for four different coverages corresponding to $N=60$, 65, 68 and 69 Xe atoms in the basic unit. Substituting Eqs. (23) in (22) gives

$$\bar{\eta}=\eta_\parallel+\frac{4}{9}\left(\frac{\pi r_0}{a}\right)^4\left(\frac{U_0}{\epsilon}\right)^2\left[\frac{\alpha_1 e_{x1}}{f_1^4}+\frac{\alpha_2 e_{x2}}{f_2^4}\right]\eta_\parallel'$$
$$=\eta_\parallel+A\eta_\parallel'.\tag{24}$$

Table 4
The frequency factors f_1 and f_2 for four different coverages

$N=60$ ($n=0.0499$ Å^{-2})	$f_1=1.9$	$f_2=1.4$
$N=65$ ($n=0.0540$ Å^{-2})	$f_1=4.2$	$f_2=3.1$
$N=68$ ($n=0.0565$ Å^{-2})	$f_1=5.7$	$f_2=4.4$
$N=69$ ($n=0.0574$ Å^{-2})	$f_1=6.2$	$f_2=4.8$

If the sliding occurs along the e_2 direction we obtain $A=9\times10^{-2}$, 4×10^{-3}, 9×10^{-4} and 6×10^{-4}, for $N=60$, 65, 68 and 69, respectively. Note that if $\eta_\parallel'\approx\eta_\parallel$ then, since $A\ll1$, the contribution from the corrugated substrate potential (proportional to U_0^2) to the sliding friction is negligible small.

Snapshot pictures of the monolayer film ($N=68$ or 69) show a nearly perfect incommensurate hexagonal structure, and it is likely that phonons in the film are very weakly damped, i.e. $\eta_\parallel''$ is very small and $\eta_\parallel'\approx\eta_\parallel$. Thus, since $A\ll1$, the contribution $A\eta_\parallel'$ to $\bar{\eta}$ will be negligible for the monolayer film, as observed in the simulations. However, snapshot pictures of the adsorbate structures for $N=65$ and $N=60$ shows that the structure has vacancy-like imperfections. (Note: these imperfections may, in fact, be an artifact of using too small a basic unit. At low temperature, for a real system a very big, nearly perfect IC solid island surrounded by a dilute 2D gas may occur instead). These will act as scattering centers for the 2D phonons in the overlayer and give rise to damping which we may estimate as $\eta_\parallel''\sim c/l$ where c is the sound velocity in the overlayer and l the phonon mean free path.

From Eq. (24) we expect $\eta_\parallel/\bar{\eta}$ to depend on $\eta_\parallel$ according to

$$\frac{\eta_\parallel}{\bar{\eta}}=\frac{\eta_\parallel}{(1+A)\eta_\parallel+A\eta_\parallel''}.$$

Thus, for "large" $\eta_\parallel$ we have $\bar{\eta}\sim\eta_\parallel$ while $\eta_\parallel/\bar{\eta}\to0$ as $\eta_\parallel\to0$. This qualitative behaviour is observed in the simulations; see Fig. 8 for two different cases, (a) $N=65$ and (b) $N=60$.

The strong rise in $\eta_\parallel/\bar{\eta}$ (see Fig. 7) and of the slip time τ (see Fig. 1) during the compression of the monolayer film is due to the very strong dependence of the phonon frequencies ω_1 and ω_2 on the spacing of the Xe atoms: when the Xe-coverage increases, ω_1 and ω_2 decreases and the contribution to $\bar{\eta}$ from the last term in (21) decreases.

At very low coverage (lattice gas) the ratio $\eta_\parallel/\bar{\eta}$ is independent of $\eta_\parallel$. To prove this, let us note that Eq. (5) depends on the dimensionless parameter

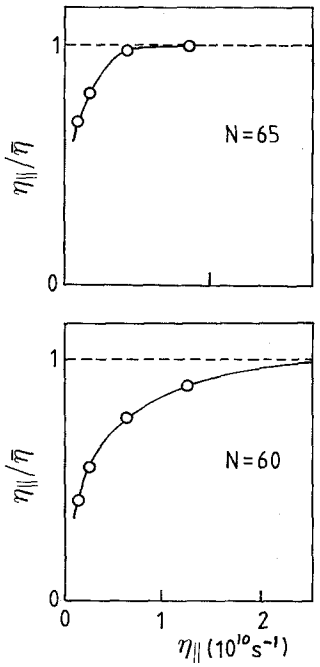

Fig. 8. The dependency of $\eta_\parallel/\bar{\eta}$ on the parallel friction $\eta_\parallel$. In the calculation for two different coverages, (a) $\theta=65/144$ and (b) 60/144. All the parameters are as in Table 1.

$\eta_\parallel/\eta_0$, where

$\eta_0=2\pi v_{\rm th}/a$.

Here, the thermal velocity $v_{\rm th}$ is defined by $v_{\rm th}=(k_{\rm B}T/m)^{1/2}\sim100$ m s^{-1} in a typical case (we have used $T=100$K and $m=131$u). No analytical solution of Eq. (5) has been presented which is valid for arbitrary $\eta_\parallel/\eta_0$, but the "high" and "low" friction limits can be treated analytically. Let us therefore estimate $\eta_\parallel/\eta_0$ in a typical experiment by Krim et al. If $a\sim2$ Å then $1/\eta_0\sim10^{-13}$ s and $\eta_\parallel/\eta_0\sim10^{-4}$ if $\eta_\parallel\sim10^9$ s^{-1}. Hence, $\eta_\parallel/\eta_0\ll1$ and since typically $U_0/k_{\rm B}T\ll1$ the low-friction limit should prevail in the experiments by Krim et al. Within linear response and for low friction, Risken and Vollmer [26] have shown that

$\bar{\eta}=\eta_\parallel I(U_0/k_{\rm B}T)$,

where

$$I(\xi)=\frac{1}{4\pi^{3/2}}\frac{\int_0^{2\pi}\mathrm{d}x\mathrm{e}^{\xi(1+\cos x)}}{\int_0^\infty\mathrm{d}\epsilon\,\dfrac{\mathrm{e}^{-\epsilon}}{\int_0^{2\pi}\mathrm{d}x[\epsilon+\xi(1+\cos x)]^{1/2}}}\qquad(25)$$

Note that $I \to 1$ and hence $\bar{\eta} \to \eta_\parallel$ as $U_0 \to 0$ while $I \to (4/\pi)\exp(2U_0/k_BT)$ and hence $\bar{\eta} \to (4\eta_\parallel/\pi)\exp(2U_0/k_BT)$ as $U_0 \to \infty$. In the latter case, $1/\bar{\eta}$ exhibit an activated temperature dependence.

It is interesting to note that the sliding friction Eq. (24) is a non-analytic function of U_0 at $U_0 = 0$. This implies that it is impossible to perform an expansion of the sliding friction in powers of U_0. This is likely to be true not only in the dilute limit (non-interacting particles) but more generally when the adsorbate layer is in a 2D fluid state, and an analytical calculation of the sliding friction for the fluid state is therefore likely to be extremely complicated even when U_0 is very small. However, when the adsorbate layer is in an IC solid state, then $\bar{\eta}$ is an analytical function of U_0 for $U_0 = 0$ and, for "small" U_0, it can be expanded in a power series of U_0. As shown above, the leading U_0 contribution in such an expansion is $\sim U_0^2$ it is clear from symmetry that no linear U_0 term can occur since translating the substrate by $a/2$ in the x and y directions, which is equivalent to replacing $U_0 \to -U_0$ in the original potential, will leave the sliding friction unchanged.

We have shown that the sliding friction of the monolayer and bilayer films is dominated by the electronic friction. Let us therefore briefly comment on the physical origin of the electronic friction for physisorbed atoms [23]. For inert atoms and molecules adsorbed on metal surfaces one can (approximately) distinguish between two contributions to the electronic friction associated with (i) the long-range attractive van der Waals interaction and (ii) the short-range Pauli repulsion associated with the overlap of the electron clouds of the adsorbate and the substrate. These contributions to $\eta_\parallel$ have, for Xe on Ag(111), been estimated to be [9,23] $\sim 8 \times 10^7$ s^{-1} and $\sim 6 \times 10^7$ s^{-1}, respectively. The fact that the two contributions are of similar magnitude is probably related to the fact that at the equilibrium separation the attractive and repulsive adsorbate–substrate interactions are of identical magnitude, which should result in dissipative forces of similar magnitudes.

The electronic friction for Xe on Ag(111) can be deduced from surface resistivity data [22], $\eta_\parallel \sim 3 \times 10^8$ s^{-1}. This value is a factor of ~ 2 larger than estimated above, but it is likely that a non-negligible contribution to the electronic friction comes from "chemical" effects, namely from the fact that the Xe 6s electronic resonance state is located around the vacuum energy with a tail extending down to the Fermi energy. In Ref. [9] the chemical contribution to $\eta_\parallel$ was estimated to be $\sim 1.5 \times 10^8$ s^{-1}.

In the equation of motion Eq. (5) for the adsorbate layer there appears the friction coefficient η. Thermal equilibrium properties of the adsorbate layer do not depend on η, but non-equilibrium properties, such as the sliding friction, depend on this parameter. In a recent paper Cieplak et al. [11] have presented a computer simulation study of the sliding of adsorbate layers on smooth substrates. Cieplak et al. claim that the sliding friction do not depend on the nature of thermal interaction between the sliding film and the substrate, e.g., they claim that the results does not depend on the microscopic friction η. In particular, they put $\eta_\parallel = 0$, i.e. they only included perpendicular friction. Our earlier results [4] and the present study cast doubt on this procedure, at least for the low-corrugation surfaces employed here. In particular, for the Xe/Ag system studied here we have found that for the incommensurate solid monolayer film the sliding friction equals $\eta_\parallel$ to a very good approximation.

7. Summary and conclusion

We have presented a computer-simulation study of the force required to slide xenon monolayer and bilayers on a silver surface. For the monolayer film we found that the sliding friction $\bar{\eta}$ is nearly identical to the parallel microscopic friction $\eta_\parallel$ (of electronic origin) which enters in the Langevin equation, while the sliding friction for the bilayer film is about 20% larger than the microscopic friction. For monolayer coverage (and below) the motion of the adsorbates perpendicular to the surface is irrelevant and a 2D model gives nearly the same result for the sliding friction as a 3D model.

In the light of our theoretical results we discussed the recent QCM measurements by Krim and Daly

[10] of the sliding friction of monolayer and bilayers of Xe on Ag(111). We conclude that for the compressed monolayer film the sliding friction is mainly of electronic origin. For the bilayer film a small fraction of the observed sliding friction may arise from internal excitations in the film, and the rest from the direct energy transfer to the substrate via the electronic friction.

Finally, we would like to emphasize that the present study has been performed for a perfect surface with no defects. It remains to study the influence of various types of defects on the sliding dynamics.

Acknowledgements

We would like to thank J. Krim, J.B. Sokoloff and Ch. Wöll for useful discussions. A.N. would like to thank the Humboldt Foundation for making it possible to spend time in Germany under the Humboldt Award Program, and KFA for hospitality.

References

[1] F.P. Bowden and D. Tabor, Friction and Lubrication (Methuen, London, 1967) pp. 17, 18; J.F. Archard, Proc. R. Soc. London Ser. A 243 (1957) 190.
[2] B.N.J. Persson and E. Tosatti, Phys. Rev. B 50 (1994) 5590.
[3] J.N. Israelachvili, Surf. Sci. Rep. 14 (1992) 109.
[4] B.N.J. Persson, Phys. Rev. B 48 (1993) 18140.
[5] A.I. Volokitin and B.N.J. Persson, in: Inelastic Energy Transfer in Interactions with Surfaces and Adsorbates, Eds. B. Gumhalter, A.C. Levi and F. Flores (World Scientific, Singapore, 1993) pp. 217–248.
[6] B.J. Hinch, A. Lock, H.H. Madden, J.P. Toennies and G. Witte, Phys. Rev. B 42 (1990) 1547; F. Hofmann and J.P. Toennies, Chem. Rev., in press.
[7] J. Krim, D.H. Solina and R. Chiarello, Phys. Rev. Lett. 66 (1991) 181.
[8] C. Holzapfel, W. Akemann, D. Schumacher, Surf. Sci. 227 (1990) 123; H. Grabhorn, A. Otto, D. Schumacher and B.N.J. Persson, Surf. Sci. 264 (1992) 327.
[9] B.N.J. Persson, Phys. Rev. B 44 (1991) 3277.
[10] J. Krim and C. Daly, in Physics of Sliding Friction, Eds. B.N.J. Persson and E. Tosatti (Kluwere, Dordrecht, 1996); C. Daly and J. Krim, Phys. Rev. Lett. 76 (1996) 803.
[11] M. Cieplak, E.D. Smith and M.O. Robbins, Science 265 (1994) 1209.
[12] J. Krim and A. Widom, Phys. Rev. B 38 (1988) 12184.
[13] M. Rodahl and B. Kasemo, Sensors Actuators, to be published.
[14] B.N.J. Persson, Sliding Friction (Springer, Berlin), to be published.
[15] J. Braun, D. Fuhrmann and Ch. Wöll, to be published.
[16] B.N.J. Persson and R. Ryberg, Phys. Rev. B 32 (1985) 3586.
[17] S. Aubry and C. Andry, Proc. Israel Physical Society, Vol. 3, Ed. C.G. Kupere (Hilger, Bristol, 1979) p. 133.
[18] J.B. Sokoloff, Phys. Rev. B 42 (1990) 760.
[19] Abramovitz and Stegun, Handbook of Mathematical Functions (1964) p. 953.
[20] J.C. Tully, G.H. Gilmer and M. Shugard, J. Chem. Phys. 71 (1979) 1630.
[21] P. Dai, T. Angot, S.N. Erlich, S.-K. Wang and H. Taub, Phys. Rev. Lett. 72 (1994) 685.
[22] C. Holzapfel, F. Stubenrauch, D. Schumacher and A. Otto, Thin Solid Films 188 (1990) 7.
[23] B.N.J. Persson and A.I. Volokitin, J. Chem. Phys. 103 (1995) 8679; See also W.L. Schaich and J. Harris, J. Phys. F 11 (1981) 65; J.B. Sokoloff, Phys. Rev. B 52 (1995) 5318.
[24] B.N.J. Persson, J. Chem. Phys. 103 (1995) 3849.
[25] J.B. Sokoloff, J. Appl. Phys. 72 (1992) 1262.
[26] H. Risken and H.D. Vollmer, Phys. Lett. A 69 (1979) 387.